Communication

Enzyme-Instructed Assembly and Disassembly Processes for Targeting Down-Regulation in Cancer Cells

Zhaoqianqi Feng, Huaimin Wang, Rong Zhou, Jie Li, and Bing Xu

J. Am. Chem. Soc., **Just Accepted Manuscript** • DOI: 10.1021/jacs.7b00070 • Publication Date (Web): 03 Mar 2017

Enzyme-Instructed Assembly and Disassembly Processes for Targeting Down-Regulation in Cancer Cells

Zhaoqianqi Feng, Huaimin Wang, Rong Zhou, Jie Li and Bing Xu*

Department of Chemistry, Brandeis University, 415 South Street, Waltham, Massachusetts 02454, United States.

Supporting Information Placeholder

ABSTRACT: Cancer cells differ from normal cells in both gain-of-functions (i.e., upregulation) and loss-of-functions (i.e., down-regulation). While it is common to suppress gain-of-function for chemotherapy, it remains challenging to target down-regulation in cancer cells. Here we show the combination of enzyme-instructed assembly and disassembly to target down-regulation in cancer cells by designing peptidic precursors as the substrates of both carboxylesterases (CES) and alkaline phosphatases (ALP). The precursors turn into self-assembling molecules to form nanofibrils upon dephosphorylation by ALP, but CES-catalyzed cleavage of ester bond on the molecules results in the disassembly of nanofibrils. The precursors selectively inhibit the cancer cells (e.g., OVSAHO) that down-regulates CES, but are innocuous to a hepatocyte (HepG2) that overexpresses CES, while both the cell lines exhibit comparable ALP activities. This work illustrates a potential approach for the development of chemotherapy via targeting down-regulation (or loss-of-functions) in cancer cells.

While the self-assembly of small molecules is a well-studied phenomenon in organic solvents[1] or on surfaces,[2] the formation of such structures in biological systems has only recently been described.[3,4,5] At the intersection of supramolecular chemistry and cell biology, supramolecular assemblies have shown great promises for cell cultures,[6] modulating immune responses,[7] delivering drugs,[8] inhibiting drug-resistant pathogens,[9] and inhibiting cancer cells.[10] We are particularly interested in the use of assemblies of molecules for cancer therapy because a serendipitous discovery[11] of the inverse comorbidity between cancer and neurodegenerative diseases implicates molecular nanofibrils formed by self-assembly inhibiting cancer cells, either in animal model[12] or in a human trial.[13] This notion, indeed, is supported by the development of enzyme-instructed self-assembly (EISA),[14] which selectively generates nanoscale assemblies of small molecules (e.g., small peptide derivatives[5,15,16] or carbohydrate derivatives[4]) *in-situ* on cancer cells for inhibiting the cancer cells.

EISA, as a process, differs fundamentally from the well-established prodrug approach[17] because, in EISA, only the assemblies, not the un-assembled products of enzymatic conversion, are inhibitory to cancer cells.[15,18] Besides acting as a multiple-step process to inhibit cancer cells,[19] EISA promises a unprecedented way for targeting down-regulation for cancer therapy, which remains a challenge in translational medicine. Scheme 1 shows the concept: A pair of cell lines both express alkaline phosphatase (ALP) in comparable levels, but one (e.g., OVSAHO) down-regulates CES, and the other (e.g., HepG2) upregulates carboxylesterase (CES). Upon the action of ALP, precursors turn into self-assembling molecules to form assemblies, but the assemblies disassociate upon the action of CES. Because the assemblies are cytotoxic and the un-assembled products are innocuous to cells, the precursors would only inhibit the cells expressing ALP and down-regulating CES. Thus, the overall result is to target the down-regulation of enzyme (e.g., CES) in cancer cells.

Scheme 1. Structures of the precursor and its hydrolysis products and the concept of targeting the cells that down-regulate CES, while expressing ALP.

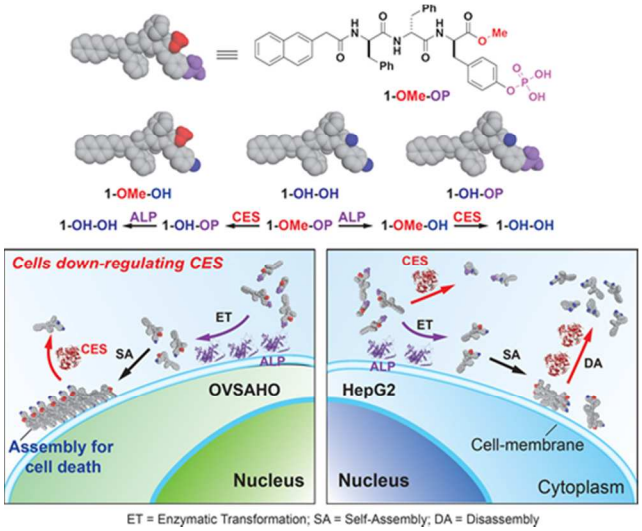

ET = Enzymatic Transformation; SA = Self-Assembly; DA = Disassembly

Based on the above concept, we design an EISA precursor **1-OMe-OP**, which contains both CES cleavage site (i.e., carboxylmethylester) and ALP cleavage site (i.e., phosphotyrosine). Such a design allows ALP to convert **1-OMe-OP** to **1-OMe-OH**, CES to turn **1-OMe-OP** into **1-OH-OP**, and the actions of ALP and CES to generate **1-OH-OH**. Critical micelle concentration (CMC) measurement and static light scattering (SLS) reveal that **1-OMe-OH** favors self-assembly. Transmission electron microscopy (TEM) confirms that **1-**

OMe-OH, generated by dephosphorylation of **1-OMe-OP**, forms nanofibrils, and CES catalyzes the dissociation of the nanofibrils by converting **1-OMe-OH** to **1-OH-OH**. Cell viability test indicates that **1-OMe-OP** potently inhibits the cancer cells (e.g., OVSAHO) that down-regulate CES, but is innocuous to the cells (e.g., HepG2) that up-regulate CES, while those two cell lines exhibit comparable phosphatase activities. Control experiments (the addition of esterase inhibitors[20]) confirm that the action and the expression level of CES are critical for selectively inhibiting the cancer cells. A dicarboxylmethylester analog of **1-OMe-OP** validates the generality of the concept. This work, for the first time, demonstrates the use of molecular assemblies to target the loss-of-function (i.e., an "untargetable" feature[21]) in cancer cells. Thus, it opens a new way for developing anticancer therapeutics based on the process of self-assembly and the down-regulation of enzymes.

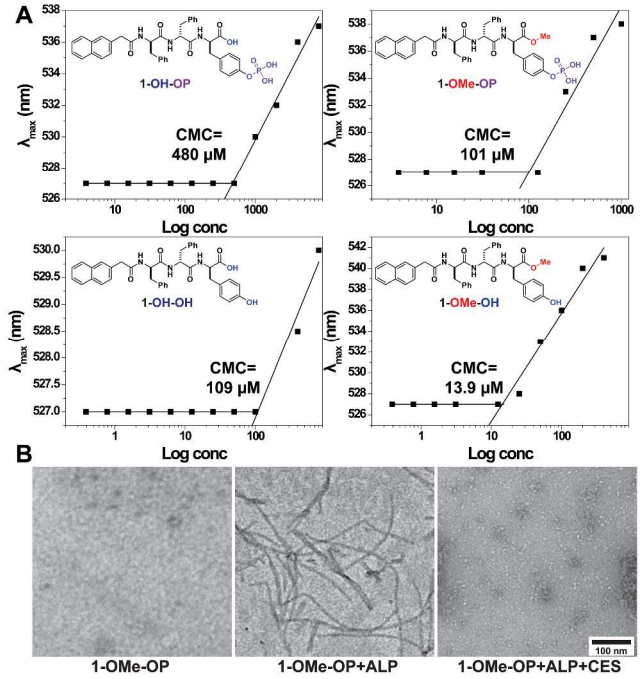

Figure 1. (A) CMCs—determination with rhodamine 6G for **1-OH-OP**, **1-OMe-OP**, **1-OH-OH**, and **1-OMe-OH**. (B) TEM of the nanostructures formed by **1-OMe-OP** (100 μM) before and after the addition of ALP or both ALP and CES. In PBS (pH 7.4) and scale bar = 100 nm.

The key feature of the design is that ALP-generated **1-OMe-OH** to form assemblies and the assemblies disassociate upon CES catalytically converting **1-OMe-OH** to **1-OH-OH**. We synthesize the precursor **1-OMe-OP** and the relevant products (**1-OMe-OH**, **1-OH-OH** and **1-OH-OP**) from its hydrolysis catalyzed by ALP or CES or both (Scheme 1). We first assess their self-assembling abilities by measure their CMCs. As shown in Figure 1A, the CMCs follow the order of **1-OMe-OH** < **1-OMe-OP** < **1-OH-OH** < **1-OH-OP**. This result indicates that the presence of phosphate group decreases self-assembling ability of the Nap-capped tripeptide (Nap-ffy), while attaching methyl group to the C-terminal of Nap-ffy increases the self-assembling ability by about an order of magnitude. We use SLS to measure the signals change upon treating **1-OMe-OP** by ALP (Figure S13). The signal intensity ratio of the solution of **1-OMe-OP** (20 μM) is 0.3. The addition of ALP to that solution increases the ratio to 98.9, but the addition of CES decreases the ratio to 0.02. Moreover, incubating **1-OMe-OP** with ALP and CES together results in **1-OH-OH** to exhibit a signal intensity ratio of 0.7, two order of magnitude lower than that of **1-OMe-OH**. Agreeing with the CMC measurement, these results indicate that CES instructs the dissociation of the assemblies formed by ALP-instructed self-assembly of **1-OMe-OH**. In addition, the TEM images (Figure 1B) show that **1-OMe-OP** hardly forms any nanostructures at the concentration of 100 μM, while the addition of ALP results in nanofibrils with a diameter of 8±2 nm. Being co-incubated with CES and ALP together, **1-OMe-OP** turns to **1-OH-OH**, which forms small particles with a diameter of 7±2 nm. These TEM images confirm that ALP instructs the assembly of **1-OMe-OH** while CES catalyzes the dissociation of the assemblies.

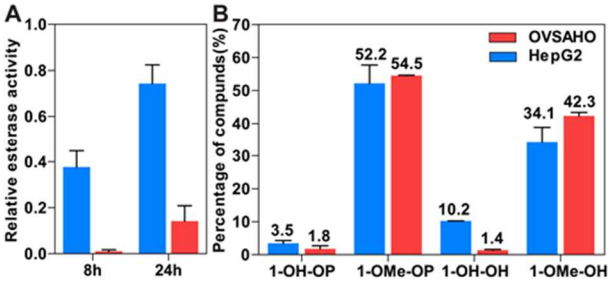

Figure 2. (A) Relative activities (comparing to culture medium) of esterase secreted from the cells. (B) Percentage of the molecular species after incubating **1-OMe-OP** (500 μM) with HepG2 or OVSAHO cells for 24 h.

To demonstrate the concept of targeting down-regulation in cellular milieu, we choose OVSAHO—an ovarian cancer cell line and HepG2—as a model cell of hepatocyte. According to the CCLE database, the mRNA expression of CES1 of HepG2 is nearly three times higher than that of OVSAHO cells, while these two cell lines express comparable levels of tissue non-specific alkaline phosphatase (ALPL) (Figure S14). Since the hydrolysis of the methylester bond in **1-OMe-OP** or **1-OMe-OH** is able to occur in pericellular space, we measure the activity of secreted esterases (Equation S1) of HepG2 or OVSAHO cells in its conditioned medium. As shown in Figure 2A, the relative activity (0.4) of the secreted esterases of HepG2 cells is almost 40 times higher than that of OVSAHO cells (0.01) at 8 hours, indicating that HepG2 cells secrete more esterases than OVSAHO cells do. In the conditioned medium of HepG2 at 24 h, the relative activity of the secreted esterases (0.7) becomes about five times of that of OVSAHO (0.14), suggesting that HepG2 cells constantly secrete more esterases than OVSAHO cells do.

We quantify the relevant conversion after incubating **1-OMe-OP** with HepG2 or OVSAHO cells for 24 h (Figure 2B). LC-MS analysis indicates that only about 50% precursors (**1-OMe-OP**) remains in both cells (i.e., 44.3 % for HepG2 and 44.2 % for OVSAHO), indicating that HepG2 and OVSAHO, in fact, exhibit comparable phosphatase activities. However, the CES from HepG2 hydrolyzes 14% of carboxylmethylester, which is four times higher than the CES from OVSAHO does (i.e., hydrolyzing 3.2 %). Although the difference of **1-OMe-OH** in HepG2 and OVSAHO is only about 8%, the molar ratios of **1-OMe-OH**/**1-OH-OH** in the cultures of HepG2 and OVSAHO are 3.3 and 30, respectively. Thus, we speculate

that **1-OH-OH** likely promotes the disassembly of **1-OMe-OH**. Congo red, a dye for self-assembled nanofibrils,[15] helps directly visualize the formation of nanofibrils in pericellular space of OVSAHO and HepG2 cells (Figure S15). Moreover, the pericellular fluorescence deceases upon washing, agreeing with that the nanofibrils form on the cell surface. The confocal images also reveal that more nanofibrils formed on OVSAHO cells than on HepG2 cells, agreeing with cell viability results. These results, agreeing with enzyme expression levels and the relative activities of the secreted esterases of the cells, further support the design (Scheme 1) for targeting cells that down-regulate CES.

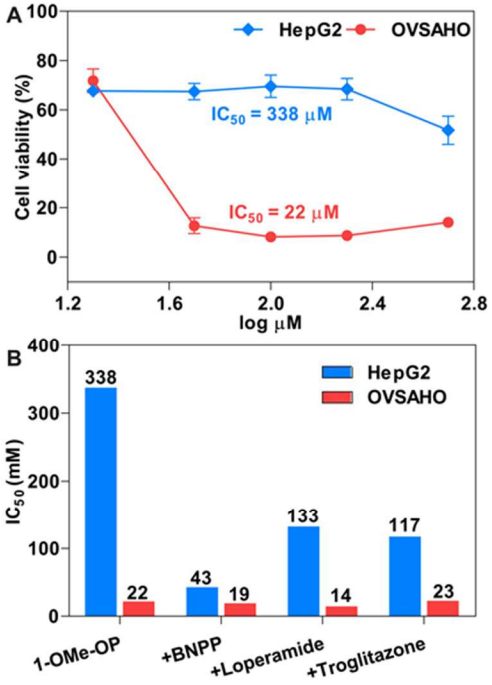

Figure 3. (A) Cell viabilities for HepG2 and OVSAHO cells treated with **1-OMe-OP**; (B) IC_{50} values (at 72 h) of **1-OMe-OP** against HepG2 or OVSAHO cells without/with addition of the inhibitors of esterases: BNPP (non-specific), loperamide (CES2) and troglitazone (CES1).

While **1-OMe-OP** potently inhibits OVSAHO cells at 50 μM (Figure 3A), it is almost innocuous to HepG2 cells. The IC_{50} value of **1-OMe-OP** against HepG2 cells (338 μM) is about fifteen times higher than that of OVSAHO cells (22 μM), confirming that **1-OMe-OP** selectively target OVSAHO cells. Besides difference in their self-assembling ability, the carboxylic species (e.g., **1-OH-OH**) likely adheres less to cell membrane than the methylester one (e.g., **1-OMe-OH**) does, thus exhibits less cytotoxicity. To prove further that CES hydrolysis contributes to the low cytotoxicity of **1-OMe-OP** against HepG2, we co-incubate CES inhibitors and **1-OMe-OP** with HepG2 (Figure 3B). The addition of troglitazone (a CES1 inhibitor[20]) or loperamide (a CES2 inhibitor[22]) reduces the IC_{50} of **1-OMe-OP** against HepG2 from 338 μM to 133 μM and 117 μM, respectively. BNPP (an inhibitor of both CES1 and CES2[23]) lowers the IC_{50} of **1-OMe-OP** against HepG2 almost an order of magnitude (from 338 μM to 43 μM). Agreeing with that HepG2 cells express both CES1 and CES2,[24] the inhibition of CES reduces the hydrolysis of **1-OMe-OH**, thus boosting the cytotoxicity of **1-OMe-OP** towards HepG2. In contrast, the addition of troglitazone hardly shows any effect on the cell viability of OVSAHO, and BNPP or loperamide only slightly decreases the IC_{50} value of **1-OMe-OP** against OVSAHO (Figure 3B, Figure S17). These results confirm that **1-OMe-OP** is able to target the down-regulation of CES in OVSAHO cells.

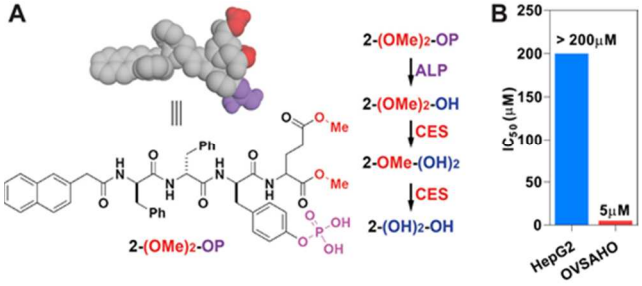

Figure 4. (A) Molecular structure and enzymatic conversion of precursor **2-(OMe)$_2$-OP**; (B) IC_{50} values (at 72 h) of **2-(OMe)$_2$-OP** against HepG2 or OVSAHO cells.

To verify the generality of the concept in Scheme 1, we develop **2-(OMe)$_2$-OP** (Figure 4A), a dicarboxylmethylester analog of **1-OMe-OP**, as another precursor (Scheme S2). Upon the action of ALP, **2-(OMe)$_2$-OP** turns into **2-(OMe)$_2$-OH**, which self-assembles in water to form nanotubes with the diameter of 14±2 nm (Figures S19 and S20). Similar to **1-OMe-OH**, **2-(OMe)$_2$-OH** becomes **2-(OH)$_2$-OH** upon the action of CES. The CMCs (Figure S21) follow the order of **2-(OMe)$_2$-OH** (2.66 μM) < **2-(OMe)$_2$-OP** (30.4 μM) < **2-(OH)$_2$-OH** (112 μM) < **2-(OH)$_2$-OP**(500 μM). Cell assays confirms that **2-(OMe)$_2$-OP** selectively inhibit OVSAHO over HepG2, exhibiting IC_{50} of 5 μM against OVSAHO cells and IC_{50} over 200 μM towards HepG2 cells (Figure 4B). Notably, the IC_{50} of **2-(OMe)$_2$-OP** is 4.4 μg/mL, comparable to cisplatin (5.5 μg/mL[25]) against OVSAHO in cell assay. Besides supporting that the molecular design of the substrates of ALP and CES (Scheme 1) is a general strategy, this result, together with the results of **1-OMe-OP**, further validate the approach of targeting the down-regulation of CES in cancer cells by enzyme-instructed assembly and disassembly processes.

In conclusion, this work demonstrates that the combination of enzyme-instructed assembly and disassembly is able to target down-regulations (or loss of function) in cancer cells. The result reported here would be particularly beneficial for treating the metastatic cancers, where the cancerous cells exist alongside healthy cells (e.g., metastatic ovarian cancer into liver[26]). Notably, the IC_{50} values of the precursors against OVSAHO cells follow the lowest CMCs of the corresponding hydrolysis products (Figure S22), indicating that the CMC values may help predict the effective concentrations of the precursors in cell assays. Interestingly, although the mRNA expression of ALPL in OVSAHO is slightly higher than that in HepG2, the two cell lines exhibit comparable phosphatase activities towards the precursors, which underscores the need to validate the enzyme activities experimentally for precisely targeting of cancer cell. Although this work uses ALP and CES, this principle demonstrated here should be applicable to any other enzymes[27] or cellular difference,[28] especially the difference in lost-of-functions, for spatiotemporal control of molecular assemblies that control cell fate.

ASSOCIATED CONTENT

Supporting Information

Synthetic procedures, characterizations, and cell viability. This material is available free of charge via the Internet at http://pubs.acs.org.

AUTHOR INFORMATION

Corresponding Author

bxu@brandeis.edu

Notes

The authors declare no competing financial interests.

ACKNOWLEDGMENT

This work was partially supported by NIH (R01CA142746) and NSF (MRSEC-1420382).

REFERENCES

(1) Terech, P.; Weiss, R. G. *Chem. Rev.* **1997**, *97*, 3133; Ikeda, A.; Shinkai, S. *Chem. Rev.* **1997**, *97*, 1713; Sangeetha, N. M.; Maitra, U. *Chem. Soc. Rev.* **2005**, *34*, 821; Lehn, J.-M. *Proc. Natl. Acad. Sci. U. S. A.* **2002**, *99*, 4763; Whitesides, G. M.; Mathias, J. P.; Seto, C. T. *Science* **1991**, *254*, 1312.

(2) Love, J. C.; Estroff, L. A.; Kriebel, J. K.; Nuzzo, R. G.; Whitesides, G. M. *Chem. Rev.* **2005**, *105*, 1103.

(3) Yang, Z.; Xu, K.; Guo, Z.; Guo, Z.; Xu, B. *Adv. Mater.* **2007**, *19*, 3152; Zorn, J. A.; Wille, H.; Wolan, D. W.; Wells, J. A. *J. Am. Chem. Soc.* **2011**, *133*, 19630; Kato, M.; Han, T. N. W.; Xie, S. H.; Shi, K.; Du, X. L.; Wu, L. C.; Mirzaei, H.; Goldsmith, E. J.; Longgood, J.; Pei, J. M.; Grishin, N. V.; Frantz, D. E.; Schneider, J. W.; Chen, S.; Li, L.; Sawaya, M. R.; Eisenberg, D.; Tycko, R.; McKnight, S. L. *Cell* **2012**, *149*, 753.

(4) Pires, R. A.; Abul-Haija, Y. M.; Costa, D. S.; Novoa-Carballal, R.; Reis, R. L.; Ulijn, R. V.; Pashkuleva, I. *J. Am. Chem. Soc.* **2015**, *137*, 576.

(5) Tanaka, A.; Fukuoka, Y.; Morimoto, Y.; Honjo, T.; Koda, D.; Goto, M.; Maruyama, T. *J. Am. Chem. Soc.* **2015**, *137*, 770.

(6) Silva, G. A.; Czeisler, C.; Niece, K. L.; Beniash, E.; Harrington, D. A.; Kessler, J. A.; Stupp, S. I. *Science* **2004**, *303*, 1352.

(7) Rudra, J. S.; Tian, Y. F.; Jung, J. P.; Collier, J. H. *Proc. Natl. Acad. Sci. U. S. A.* **2010**, *107*, 622; Wang, H. M.; Luo, Z.; Wang, Y. C. Z.; He, T.; Yang, C. B.; Ren, C. H.; Ma, L. S.; Gong, C. Y.; Li, X. Y.; Yang, Z. M. *Adv. Funct. Mater.* **2016**, *26*, 1822.

(8) Zhao, F.; Ma, M. L.; Xu, B. *Chem. Soc. Rev.* **2009**, *38*, 883; Cheetham, A. G.; Zhang, P.; Lin, Y.-a.; Lock, L. L.; Cui, H. *J. Am. Chem. Soc.* **2013**, *135*, 2907.

(9) Salick, D. A.; Kretsinger, J. K.; Pochan, D. J.; Schneider, J. P. *J. Am. Chem. Soc.* **2007**, *129*, 14793; Xing, B. G.; Yu, C. W.; Chow, K. H.; Ho, P. L.; Fu, D. G.; Xu, B. *J. Am. Chem. Soc.* **2002**, *124*, 14846.

(10) Julien, O.; Kampmann, M.; Bassik, M. C.; Zorn, J. A.; Venditto, V. J.; Shimbo, K.; Agard, N. J.; Shimada, K.; Rheingold, A. L.; Stockwell, B. R.; Weissman, J. S.; Wells, J. A. *Nat. Chem. Biol.* **2014**, *10*, 969.

(11) Driver, J. A.; Beiser, A.; Au, R.; Kreger, B. E.; Splansky, G. L.; Kurth, T.; Kiel, D. P.; Lu, K. P.; Seshadri, S.; Wolf, P. A. *Br. Med. J.* **2012**, *344*.

(12) Gallardo, R.; Ramakers, M.; De Smet, F.; Claes, F.; Khodaparast, L.; Khodaparast, L.; Couceiro, J. R.; Langenberg, T.; Siemons, M.; Nystrom, S.; Young, L. J.; Laine, R. F.; Young, L.; Radaelli, E.; Benilova, I.; Kumar, M.; Staes, A.; Desager, M.; Beerens, M.; Vandervoort, P.; Luttun, A.; Gevaert, K.; Bormans, G.; Dewerchin, M.; Van Eldere, J.; Carmeliet, P.; Vande Velde, G.; Verfaillie, C.; Kaminski, C. F.; De Strooper, B.; Hammarstrom, P.; Nilsson, K. P. R.; Serpell, L.; Schymkowitz, J.; Rousseau, F. *Science* **2016**, *354*, 720.

(13) Gustafsson, L.; Leijonhufvud, I.; Aronsson, A.; Mossberg, A.-K.; Svanborg, C. *N. Engl. J. Med.* **2004**, *350*, 2663.

(14) Du, X.; Zhou, J.; Shi, J.; Xu, B. *Chem. Rev.* **2015**, *115*, 13165.

(15) Kuang, Y.; Shi, J.; Li, J.; Yuan, D.; Alberti, K. A.; Xu, Q.; Xu, B. *Angew. Chem., Int. Ed.* **2014**, *53*, 8104.

(16) Wang, H.; Feng, Z.; Wu, D.; Fritzsching, K. J.; Rigney, M.; Zhou, J.; Jiang, Y.; Schmidt-Rohr, K.; Xu, B. *J. Am. Chem. Soc.* **2016**, *138*, 10758; Feng, Z.; Wang, H.; Du, X.; Shi, J.; Li, J.; Xu, B. *Chem. Commun.* **2016**, *52*, 6332; Li, J.; Kuang, Y.; Shi, J. F.; Zhou, J.; Medina, J. E.; Zhou, R.; Yuan, D.; Yang, C. H.; Wang, H. M.; Yang, Z. M.; Liu, J. F.; Dinulescu, D. M.; Xu, B. *Angew. Chem., Int. Ed.* **2015**, *54*, 13307; Wang, H. M.; Feng, Z. Q. Q.; Wang, Y. Z.; Zhou, R.; Yang, Z. M.; Xu, B. *J. Am. Chem. Soc.* **2016**, *138*, 16046.

(17) Rautio, J.; Kumpulainen, H.; Heimbach, T.; Oliyai, R.; Oh, D.; Jaervinen, T.; Savolainen, J. *Nat. Rev. Drug Discovery* **2008**, *7*, 255; Brunton, L.; Hilal-Dandan, R.; Goodman, L. S. *Goodman and Gilman manual of pharmacology and therapeutics*; Mcgraw Hill Professional: New York, **2013**.

(18) Shi, J.; Du, X.; Yuan, D.; Zhou, J.; Zhou, N.; Huang, Y.; Xu, B. *Biomacromolecules* **2014**, *15*, 3559.

(19) Zhou, J.; Xu, B. *Bioconjugate Chem.* **2015**, *26*, 987.

(20) Fu, J.; Sadgrove, M.; Marson, L.; Jay, M. *Drug Metab. Dispos.* **2016**, *44*, 1313.

(21) Bourzac, K. *Nature* **2014**, *509*, S69.

(22) Quinney, S. K.; Sanghani, S. P.; Davis, W. I.; Hurley, T. D.; Sun, Z.; Murry, D. J.; Bosron, W. F. *J. Pharmacol. Exp. Ther.* **2005**, *313*, 1011.

(23) Ohura, K.; Sakamoto, H.; Ninomiya, S.-i.; Imai, T. *Drug Metab. Dispos.* **2010**, *38*, 323.

(24) Ross, M. K.; Borazjani, A.; Wang, R.; Crow, J. A.; Xie, S. *Arch. Biochem. Biophys.* **2012**, *522*, 44.

(25) Elias, K. M.; Emori, M. M.; Papp, E.; MacDuffie, E.; Konecny, G. E.; Velculescu, V. E.; Drapkin, R. *Gynecol. Oncol.* **2015**, *139*, 97.

(26) Langyel, E. *Am. J. Pathol.* **2010**, *177*, 1053.

(27) Dragulescu-Andrasi, A.; Kothapalli, S. R.; Tikhomirov, G. A.; Rao, J. H.; Gambhir, S. S. *J. Am. Chem. Soc.* **2013**, *135*, 11015; Jiang, T.; Olson, E. S.; Nguyen, Q. T.; Roy, M.; Jennings, P. A.; Tsien, R. Y. *Proc. Natl. Acad. Sci. U. S. A.* **2004**, *101*, 17867.

(28) Zheng, Z.; Chen, P.; Xie, M.; Wu, C.; Luo, Y.; Wang, W.; Jiang, J.; Liang, G. *J. Am. Chem. Soc.* **2016**, *138*, 11128.

Insert Table of Contents artwork here